European Journal of Pharmaceutics and Biopharmaceutics 74 (2010) 193–201

Contents lists available at ScienceDirect

European Journal of Pharmaceutics and Biopharmaceutics

journal homepage: www.elsevier.com/locate/ejpb

Research paper

Cyclodextrin-based nanosponges encapsulating camptothecin: Physicochemical characterization, stability and cytotoxicity

Shankar Swaminathan [a,e], Linda Pastero [b], Loredana Serpe [c], Francesco Trotta [d], Pradeep Vavia [e], Dino Aquilano [b], Michele Trotta [a], GianPaolo Zara [c], Roberta Cavalli [a,*]

[a] Dipartimento di Scienza e Tecnologia del Farmaco, Università degli Studi di Torino, Italy
[b] Dipartimento di Scienze Mineralogiche e Petrologiche, Università degli Studi di Torino, Italy
[c] Dipartimento di Anatomia, Farmacologia e Medicina Legale, Università degli Studi di Torino, Italy
[d] Dipartimento di Chimica IFM, Università degli Studi di Torino, Italy
[e] Centre for Novel Drug Delivery System, Institute of Chemical Technology, University of Mumbai, India

ARTICLE INFO

Article history:
Received 29 May 2009
Accepted in revised form 4 November 2009
Available online 10 November 2009

Keywords:
Nanosponges
Camptothecin
β-Cyclodextrin
Crystallinity
Stability
Complexation
Cytotoxicity

ABSTRACT

Camptothecin (CAM), a plant alkaloid and a potent antitumor agent, has a limited therapeutic utility because of its poor aqueous solubility, lactone ring instability and serious side effects. Cyclodextrin-based nanosponges (NS) are a novel class of cross-linked derivatives of cyclodextrins. They have been used to increase the solubility of poorly soluble actives, to protect the labile groups and control the release. This study aimed at formulating complexes of CAM with three types of β-cyclodextrin NS obtained with different cross-linking ratio (viz. 1:2, 1:4 and 1:8 on molar basis with the cross-linker) to protect the lactone ring from hydrolysis and to prolong the release kinetics of CAM. Crystalline ($F_{1:2}$, $F_{1:4}$ and $F_{1:8}$) and paracrystalline NS formulations were prepared. XRPD, DSC and FTIR studies confirmed the interactions of CAM with NS. XRPD showed that the crystallinity of CAM decreased after loading. CAM was loaded as much as 21%, 37% and 13% w/w in $F_{1:2}$, $F_{1:4}$ and $F_{1:8}$, respectively while the paracrystalline NS formulations gave a loading of about 10% w/w or lower. The particle sizes of the loaded NS formulations were between 450 and 600 nm with low polydispersity indices. The zeta potentials were sufficiently high (−20 to −25 mV) to obtain a stable colloidal nanosuspension. The *in vitro* studies indicated a slow and prolonged CAM release over a period of 24 h. The NS formulations protected the lactone ring of CAM after their incubation in physiological conditions at 37 °C for 24 h with a 80% w/w of intact lactone ring when compared to only around 20% w/w of plain CAM. The cytotoxicity studies on HT-29 cells showed that the CAM formulations were more cytotoxic than plain CAM after 24 h of incubation.

1. Introduction

Cyclodextrin-based nanosponges (NS) are hyper-cross-linked cyclodextrins synthesized by the procedure mentioned elsewhere [1]. Briefly, NS can be obtained by cross-linking different types of cyclodextrins (CD) with a carbonyl or a dicarboxylate compound as cross-linker. They are solid particles with a spherical morphology that have been reported to have a very high solubilizing power for poorly soluble molecules [2], and they are proposed to form inclusion and non-inclusion complexes with different drugs [3–6]. The CD cross-linker ratio can be varied during their preparation to improve the drug loading and to obtain a tailored release profile.

A previous work dealing with β-CD-based nanosponges focused on the solubilization of molecules for immediate release [4]. Herein, we propose NS application for protection of active molecules from physicochemical degradation and for sustained release.

Camptothecin (CAM), a plant alkaloid, is a potent anticancer agent acting through the inhibition of topoisomerase I during the S-phase of the cell cycle [7]. CAM and its derivatives have shown a wide spectrum of anticancer activity against human malignancies including human lung, prostate, breast, colon, stomach, ovarian carcinomas, melanoma, lymphomas and sarcomas [8–10]. After its isolation and characterization in 1966 by Wall et al. [11] from the oriental tree *Camptotheca acuminata*, it roused a tremendous interest due to its unprecedented antitumor activity, but failed to live to its expectations due to problems associated with serious toxic side effects. The interest was rekindled in the early 1990s when it was found that unlike many other antitumor agents, which inhibit cancer cell proliferation by binding to DNA, CAM acted by binding to the topoisomerase I–DNA complex, thereby causing accumulation of DNA strand breaks upon replication, leading to cell death [12]. Despite of this high activity, it has a limited

* Corresponding author. Tel.: +39 011 6707825; fax: +39 011 6707687.
E-mail address: roberta.cavalli@unito.it (R. Cavalli).

0939-6411/$ - see front matter © 2009 Elsevier B.V. All rights reserved.
doi:10.1016/j.ejpb.2009.11.003

therapeutic utility. This is due to its poor aqueous solubility, serious side effects and opening of the lactone ring at physiological pH to yield the carboxylate form which is inactive [13,14]. In addition, the ring-opening results in charged drug species exhibiting limited permeability through the lipid bilayer of a low dielectric constant, thereby altering the molecular diffusivity [15].

Extensive researches have been carried out to develop delivery systems for the insoluble lactone form of CAM and its derivatives [16]. These include entrapment into liposomes, microspheres or nanoparticles, complexation with lipids or cyclodextrins and preparation of macromolecular prodrugs.

This work focused on the development of new formulations for CAM which consist of the encapsulation in nanosponges for prolonging the shelf life and the release of the drug. The nanosponges may solubilize CAM by complexation and may protect the lactone ring from opening due to its high inclusion abilities thereby increasing the drug stability.

2. Materials and methods

2.1. Materials

β-CD was a generous gift from Wacker Chemie, (Munich, Germany). Diphenyl carbonate and CAM were purchased from Sigma–Aldrich (Milan, Italy). All other chemicals and reagents were of analytical grade. Milli Q water (Millipore) was used throughout the studies.

2.2. Synthesis of β-CD nanosponges

A series of three types of β-CD NS was prepared using diphenylcarbonate for the cross-linking as previously reported [1]. Briefly, an amount of anhydrous cyclodextrin was put to react in melted diphenylcarbonate at 90 °C for at least 5 h. Then, the solid was ground in a mortar and Sohxlet extracted with ethanol to remove either impurities or unreacted diphenylcarbonate. The reaction was carried out using a cross-linker excess, at three different molar ratios, e.g. 1:2, 1:4, 1:8 (β-CD:cross-linker). After purification, NS were stored at 25 °C until further use. This reaction was also carried out in the presence of ultrasound, and two different types of NS, namely, crystalline (1:2 NS, 1:4 NS, 1:8 NS) and paracrystalline (1:2, 1:4, or 1:8 NS_{para}), were formed based on the process conditions of the synthesis.

2.3. Preparation of CAM-loaded nanosponges

CAM was dispersed in aqueous suspensions of the various types of nanosponges in a ratio of 1:4 (drug to NS by weight) and was stirred for 24 h in the dark and at acidic pH to avoid the formation of the carboxylate form of camptothecin. After 24 h, the suspensions were centrifuged at 2000 rpm for 10 min to separate the uncomplexed drug as a residue below the colloidal supernatant. The colloidal supernatants were freeze-dried to obtain drug-loaded NS formulations, named as $F_{1:2}$, $F_{1:4}$ and $F_{1:8}$ and F_{para}, depending upon the ratio of β-CD:cross-linker. The drug-loaded NS formulations were stored in a covered vacuum desiccator at room temperature until further use.

2.4. Preparation of CAM physical mixtures

Binary physical mixtures of the series of nanosponges with the drug were prepared by mixing appropriate amounts of solid components (4:1 NS:CAM weight ratio) in a glass mortar.

2.5. Determination of CAM loading in nanosponges

Weighed amount of loaded nanosponges were dispersed in a methanol:chloroform mixture (1:4 v/v), suitably diluted in methanol and were analyzed by HPLC. Briefly, a Shimadzu instrument model no. LC-9A, equipped with C R5A cromatopac integrator and RF-551 spectrofluorometric detector in isocratic conditions was used. The separation was carried out using an octadecylsilane column with a 5 μm pore size with a mobile phase containing acetonitrile and triethanolamine aqueous solution (1% w/v) in a ratio of 35:65 (v:v) using a fluorescent detector at a λ_{ex} = 360 nm and λ_{em} = 440 nm. The flow rate was kept at 0.8 ml/min. The peak of CAM (lactone) was obtained at a retention time of about 9 min and that of carboxylate form (if present) was obtained at a retention time of about 3 min. The standard solutions of CAM-lactone and CAM-carboxylate for the calibration curves were made by dilution of the CAM stock solution in dimethylsulfoxide. The analysis of the carboxylate form was carried out 24 h after preparing the solution in NaOH 0.1 N to ensure the complete conversion of the CAM-lactone to the carboxylate forms. The calibration curves were linear in the range 0.1–0.5 μg/ml.

2.6. Physicochemical characterization of CAM-loaded nanosponges

2.6.1. Fourier Transform Infrared spectroscopy (FTIR)

It was performed, using a Perkin Elmer system 2000 spectrophotometer, to understand if there exists some interaction between drug and NS. The spectra were obtained on KBr pellets in the region from 4000 cm^{-1} to 650 cm^{-1}.

2.6.2. Differential scanning calorimetry (DSC)

It was carried out by means of a Perkin Elmer DSC/7 differential scanning calorimeter (Perkin-Elmer, CT-USA) equipped with a TAC 7/DX instrument controller. The instrument was calibrated with indium for melting point and heat of fusion. A heating rate of 10 °C/min was employed in the 25–300 °C temperature range. Standard aluminum sample pans (Perkin-Elmer) were used; an empty pan was used as reference standard. Analyses were performed in triplicate on 5 mg samples under nitrogen purge.

2.6.3. X-ray powder diffraction (XRPD)

To characterize the nanosponges and the CAM complexes, we carried out a detailed XRPD study using both a Huber Guinier Camera G670 (simultaneous collection of reflections between 7° and 100° 2θ) and a Siemens D5000 diffractometer (Bragg–Brentano geometry, sequential collection between 2.5° and 60° 2θ).

2.6.4. Size, polydispersity index and zeta potential values

NS sizes and polydispersity indices were measured by dynamic light scattering using a 90 Plus particle sizer (Brookhaven Instruments Corporation, USA) equipped with MAS OPTION particle sizing software. The measurements were made at a fixed angle of 90° for all samples and 25 °C. The samples were suitably diluted with filtered distilled water for every measurement. Zeta potential measurements were also made using an additional electrode in the same instrument. For zeta potential determination, samples of the three formulations were diluted with 0.1 mM KCl and placed in the electrophoretic cell, where an electric field of about 15 V/cm was applied.

2.6.5. Optical microscopy (OM)

The NS suspensions were observed using a Leitz invert microscope after suitable dilution with water and saline solution to evaluate the effect of the dilution on the NS formulations. The OM was also used to investigate the morphology of erythrocytes after the incubation with the NS.

2.6.6. Transmission electron microscopy (TEM)

It was employed to evaluate the particle shape and size A Philips CM 10 transmission electron microscope was used, and the particle size was measured using the NIH image software. The nanosponge suspensions were sprayed on Formwar-coated copper grid and air-dried before observation.

2.7. In vitro release of CAM from nanosponge formulations

The *in vitro* release was carried out using multi-compartment rotating cells with a dialysis membrane (Sartorius, cut off 12,000 Da). The donor phase consisted of formulations containing a fixed amount of CAM in phosphate buffer at pH 7.4 (1 ml). The receiving phase consisted of phosphate buffer, pH 7.4 added with 0.5% w/v sodium lauryl sulfate (1 ml) to maintain proper sink conditions. The receiving phase was completely withdrawn and replaced with fresh medium after fixed time intervals, suitably diluted and analyzed using the HPLC method described previously. Glacial acetic acid (50 μl/ml of sample) was added to the samples that were frozen at −18 °C until analysis to avoid conversion of lactone form to carboxylate form. The experiment was carried out in triplicate.

2.8. Stability determination of CAM in physiological conditions

CAM and its formulations were subjected to short-time stability studies (24 h) in PBS solution (pH 7.4) and in fresh human plasma (diluted suitably with PBS) at 37 °C. Formulations containing equal amounts of CAM (200 μg/ml) were dispersed in both media and were mixed uniformly using a cyclo-mixer. An aliquot of each suspension was taken, and the amount of CAM (either lactone or carboxylate form) was determined using the HPLC method previously described. After 24 h, CAM (both forms) was again determined. The amounts of lactone and carboxylate forms were expressed in % w/w in each formulation in comparison with CAM.

2.9. Haemolytic activity of CAM formulations

CAM formulations (equivalent to 200 μg/ml of CAM) were incubated at 37 °C for 90 min with 1 ml of diluted blood. Freshly prepared PBS (pH 7.4) was used for all dilution purposes.

After incubation, blood containing suspensions were centrifuged at 2000 rpm for 10 min to separate plasma. The amount of haemoglobin released due to haemolysis was measured spectrophotometrically at 543 nm (Du 730, Beckman). The haemolytic activity was calculated with reference to blank and complete haemolyzed samples (induced by addition of ammonium sulfate 20% w/v). Optical microscopy was also used to see if there were any abnormalities in the blood cells after incubation. The observations were made with reference to the blank diluted blood.

2.10. In vitro cytotoxicity of CAM formulations

The human colorectal adenocarcinoma cell line, HT-29, was obtained from the American Type Culture Collection (Rockville, MD, USA). HT-29 cells were grown as a monolayer culture in RPMI 1640 medium supplemented with 10% heat-inactivated fetal calf serum (FCS), 2 mmol/l L-glutamine and penicillin/streptomycin (100 units/ml), at 37 °C in 5% CO_2 humidified atmosphere. At the beginning of the experiments, cells in exponential growth phase were removed from the flasks with 0.05% trypsin–0.02% EDTA solution. Cells were seeded in 24 wells/plate (25,000 cells/well) in RPMI 1640 medium with 10% FCS. The cells were allowed to attach for 72 h, and seeding medium was removed and replaced by experimental medium. Cells were maintained for 72 h in medium supplemented with increasing concentrations (from 0.01 to 10.0 μM) of CAM and 1:2, 1:4, 1:8 NS. Unloaded NS were also evaluated on HT-29 cell line growth at the highest concentration of NS used. All experiments were done two times, each condition being performed in triplicate. Cell viability was assessed by trypan blue exclusion assay. For cell experiments, NS and NS formulations were sterilized by autoclaving. CAM was solubilized in DMSO and then suitably diluted.

2.11. Statistical analysis

Statistical analysis of differences among the formulations was performed using Student's *t*-test.

A 0.05 level of probability was taken as level of significance.

3. Results and discussion

The insolubility of CAM in most of biocompatible solvents has made very difficult to deliver this drug through the conventional approaches.

Several delivery systems, as microparticles, nanoparticles, liposomes, micelles, miniemulsions, have been developed and investigated to overcome the solubility and stability problems of CAM, besides chemical modifications [16–20]. The need of a system to further improve the therapeutic efficacy of the drug and to reduce its toxic effects is continuously attracting the research attention. Different types of solid lipid nanoparticles have been developed for camptothecin delivery [21] showing a higher cytotoxicity on cells than the free control. A novel biodegradable and biocompatible camptothecin-polymer implant based on chitosan for sustained intratumoral release of the drug has been described [22]. Recently, acoustically active pefluorocarbon nanoemulsions for camptothecin encapsulation have been prepared to overcome the delivery problems [23]. The use of cyclodextrins represents another technological approach to increase drug solubility. The CAM complexation with β-cyclodextrin, γ-cyclodextrin and their derivatives has been previously investigated showing an improve in the solubility and stability of the drug [24,25]. Cyclodextrin-based nanosponges showed superior complexing ability than natural cyclodextrins towards many molecules [2].

In this study, new CAM formulations were developed using beta-CD-based nanosponges obtained by the reaction of β-cyclodextrin with diphenylcarbonate. NS are hyper-cross-linked cyclodextrin polymers consisting of solid nanoparticles with colloidal sizes and nanosized cavities. These nanostructured materials can form inclusion and non-inclusion complexes with different compounds and formed a nanosuspension of rather uniform spherical-shaped nanoparticles after dispersion in water under stirring. NS structural characterization [unpublished data] had showed that the carbonate linkage was added to the primary hydroxyl groups of the parent β-CD unit. Thus, the drug molecules could be included inside the nanocavities of β-CD and due to the cross-linking further interactions of the guest molecules with more β-CD units might be thought. Moreover, the presence of the cross-linked network might also form nanochannels in the NS structure for the polymer mesh. This peculiar structural organization might be responsible for the increased solubilization and protection capacities of nanosponges in comparison with the parent cyclodextrin.

For CAM formulation, a series of NS with varying degrees of cross-linking and crystallinity were synthesized and characterized prior to use to have uniform batches. A possible schematic structure of NS is reported in Fig. 1.

X-ray analysis was used to characterize the NS solid structure. Both plain β-CD (not cross-linked) and plain CAM showed a crystalline structure at XRPD as reported in Fig. 2.

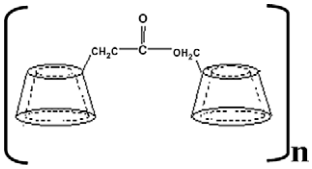

Fig. 1. Schematic structure of NS.

Due to the synthetic procedure, NS could be obtained from β-CD cross-linking reaction either in poorly crystalline (paracrystalline) or in crystalline form (Fig. 3).

In Fig. 3a, poorly crystalline NS from β-CD cross-linked (1:4 β-CD/cross-linker agent ratio) are compared with the well crystallized ones at the same cross-linker ratio. Patterned grey and white areas indicate the 2θ interval chosen for the integral area evaluation. In Fig. 3b and c, XRPD pattern decomposition shows some broad reflections in the paracrystalline phase that appear as narrow peaks in the crystalline sample.

Poorly crystalline nanosponges formed using different β-CD cross-linking ratio show very similar XRPD patterns (data not shown). But the decomposition of the XRPD diagrams of this types of paracrystalline NS underlines the crystallinity degree of the NS with a weak long range order characterized by some broad reflections indicated in Fig. 3; the short range order being almost lost and represented only by a very large peak at 34.24° (2θ).

As it comes out from the XRPD pattern decomposition, some peaks occur in the crystalline NS as well as in the nearly amorphous one, but their areas and, particularly, the intensity vs. FWHM (Full Width at Half Maximum) ratio reported in Tables 1 and 2 are clearly different, so outlining their different crystallinity.

This indicates that a deep decrease occurs in the overall crystal quality, as if the crystals transform in amorphous state. However, this is not the case, since the broadening of the peaks can be reasonably related with an outstanding decrease in crystal size owing to the variation of some crystallization parameters. In fact, as evidenced in Fig. 3, the XRPD pattern of the nanosponge paracrystalline phase can be generated from the convolution of the XRPD diagram recorded on the nanosponge crystalline phase.

Paracrystalline nanosponges showed a different loading capacity with CAM. When CAM is loaded into poorly crystalline NS, the drug complex loses its ordering, i.e. CAM loading occurs as mechanical mixture rather than inclusion complex (Fig. 4a).

On the other hand, crystalline NS show different XRPD patterns with narrow reflections and good peak/background ratio. Crystalline NS cross-linked with different amounts of cross-linking agent show a direct dependence between crystallinity and β-CD/cross-linking agent ratio (Fig. 4b). Comparing XRPD peak intensity and intensity/FWHM ratio for the diffraction peaks, the 1:2 pattern shows a higher crystallinity with respect to 1:4 and 1:8 XRPD patterns that, on the contrary, are very similar. Nevertheless, the sample with the 1:8 cross-linking ratio shows a slight decrease in the complex crystallinity. Consequently, we can suppose that the higher cross-linking degree can be found in between 1:2 and 1:4 ratios.

For low values of the CD/cross-linking agent ratio, the cross-linking process rapidly increases while, for intermediate and high values, it slowly grows without reaching a plateau.

These CAM-loaded crystalline NS show a frankly crystalline structure. When comparing their XRPD patterns with those obtained from both plain NS and plain CAM, no perfect coincidence was found. To evaluate if a new phase takes place due to chemical interactions, instead of a physical mixture between CAM and NS, some XRPD simulations were carried out on mechanical mixtures (see Fig. 4b).

In Fig. 4b, CAM, CAM–NS simulated physical mixture and CAM-loaded NS XRDP patterns were compared in order to outline the different behaviour between the experimentally obtained complexes and physical mixtures and the simulated ones. So, it was clearly proved that in the CAM-loaded nanosponges, the CAM complexation is not only due to a mechanical mixing of the components, but also CAM loading brings to the formation of a new ordered phase.

The analysis of the physical mixture confirmed this behaviour (data not shown).

Different packing of CAM in the crystal structure of NS complexes might affect physical and pharmaceutical properties of CAM as drug loading, drug stability and drug release.

The observed differences could be related to the presence of channels or cavities running through the NS crystal structure and working as sites for CAM molecules besides cyclodextrin cavities. When the crystal structure of the NS collapses, as in the case of the paracrystalline NS, the beehive-like structure of the complex fails, and the CAM molecules lose their preferential crystallographic sites. This outcome is confirmed by the CAM loading that is greater in the crystalline NS than in the paracrystalline ones.

From the HPLC analyses, it was found that for the crystalline nanosponges CAM was loaded in the highest amount in 1:4 NS as much as 37% w/w, while 21% and 13% w/w in 1:2 and 1:8 types of NS, respectively. The different CAM loading showed that the

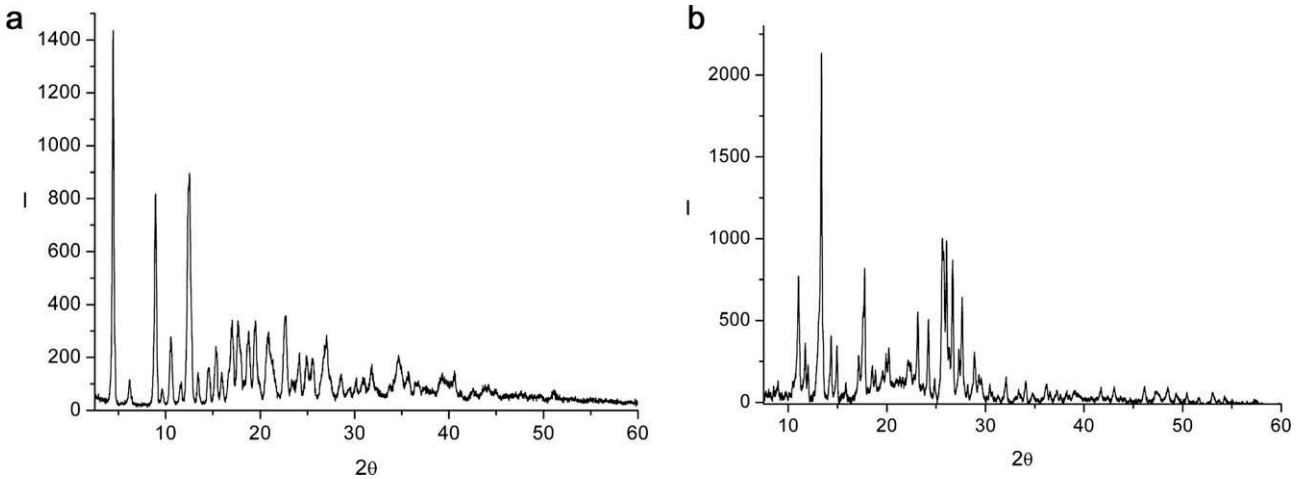

Fig. 2. XRPD pattern of (a) the plain β-CD; (b) XRPD pattern of CAM drug.

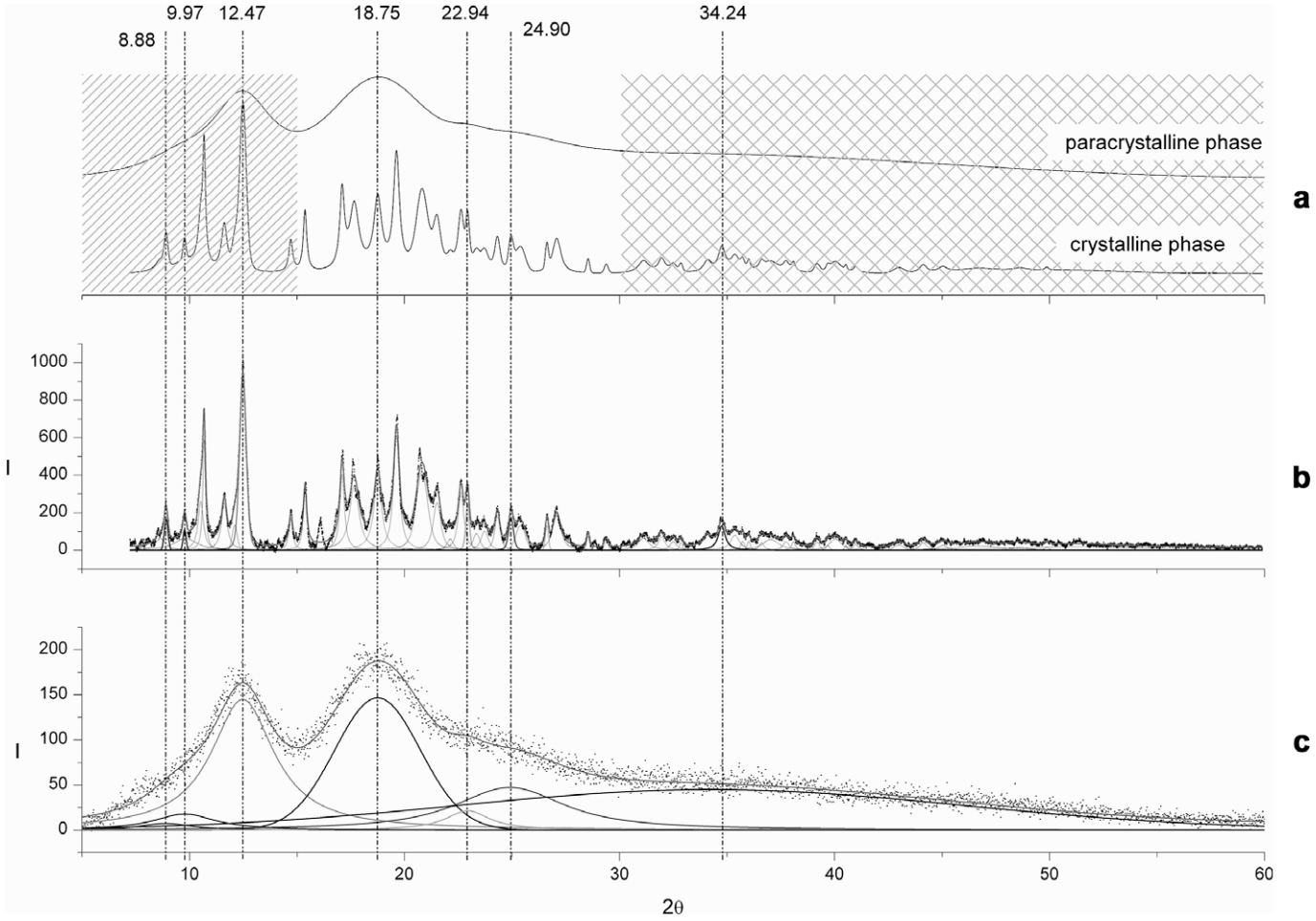

Fig. 3. (a) Poorly crystalline NS from β-CD cross-linked (1:4 β-CD/cross-linker agent ratio) compared with the well crystallized ones at the same cross-linker ratio (b). Patterned grey and white areas indicate the 2θ interval chosen for the integral area evaluation. XRPD pattern decomposition shows some broad reflections in the paracrystalline phase that appear as narrow peaks in the crystalline sample (c).

Table 1
Peak position recurrence between poorly crystalline NS sample and crystalline NS sample and intensity vs. FWHM ratios.

Peak position	Poorly crystalline sample		Crystalline sample	
(2θ)	Area	I/FWHM	Area	I/FWHM
8.88	32.23	2.59	102.56	544.26
9.77	94.80	5.10	54.36	10189.73
12.47	807.58	40.86	436.64	2343.21
18.75	731.34	31.32	330.27	792.99
22.94	80.82	8.76	49.17	3389.02
24.90	427.23	7.78	69.71	641.95
34.24	1318.59	1.62	244.04	68.93

Table 2
Areas measured over the previously indicated 2θ ranges. The multiplication factor (1.5) is closely related to the instrumental enhancement.

	2θ range (degrees)	Paracrystalline phase	Crystalline phase	Area ratio
Integral #1	7.5–15	799.1	1187.6	1.49
Integral #2	15–30	1668.3	2521.8	1.51
Integral #3	30–60	980.6	1488.7	1.52

degree of cross-linking affected the complexation ability of NS. It might be supposed that in 1:2 NS, the lower amount of cross-linker formed a network with an uncompleted cyclodextrin cross-linking and with decreased sites for the drug complexation; thus, CAM might not be included in higher amount in this types of NS. While in 1:8 NS, the higher amount of cross-linker might provide a high cross-linking of β-CD, and consequently a part of CAM interaction with β-CD cavities might be hindered.

The CAM loading in NS that did not show a specific crystal structure (NS_{para}) was lower, about 10% w/w for the 1:4 NS, suggesting that probably the crystal structure of NS plays a very important role in complexation of CAM. The role of the crystalline structure on NS complexation ability is under investigation showing its marked influence also with other types of active molecules.

The CAM complexation with nanosponges was also confirmed by FTIR and thermal analyses.

FTIR studies showed that there are weak interactions between NS and CAM that were evident from broadenings and disappearance of the drug peaks in case of complexes (Fig. 5).

The plain nanosponge FTIR spectra showed the presence of the carbonate bond which has a peak at around 1700–1750 cm^{-1}. The main characteristic peaks of CAM are at around 1750, 1460–1600, 1270–1290 cm^{-1}. These CAM characteristic peaks were broadened or shifted in the formulations suggesting definite interactions between CAM and NS. The thermal analysis of CAM-loaded nanosponges confirmed the drug complexation.

DSC thermograms of the complexes did not show the melting peak corresponding to drug fusion; this indicates that the drug is

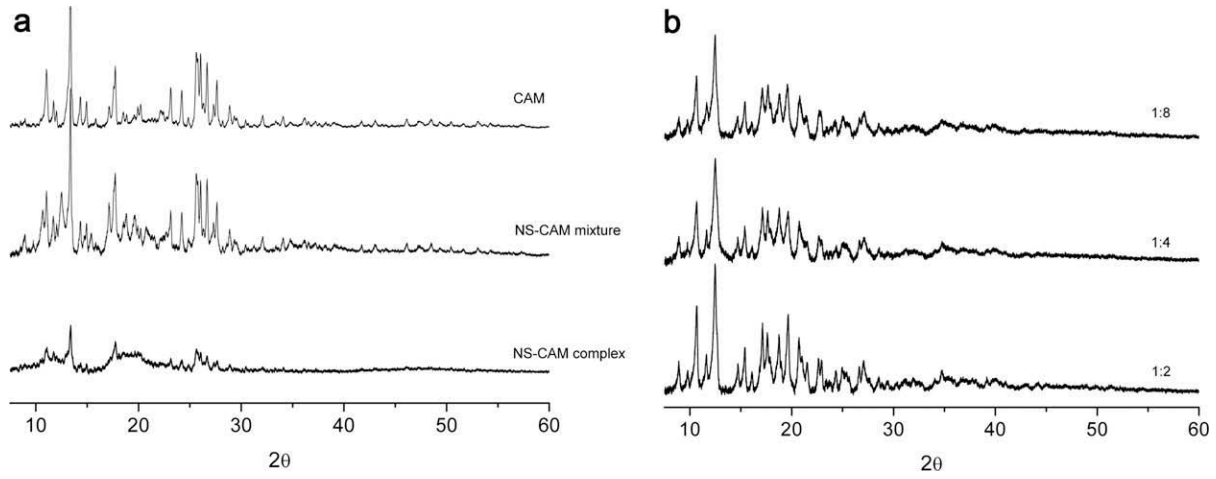

Fig. 4. (a) X-ray diagrams of crystalline CAM-loaded NSs (CAM-NS complex) compared with pure CAM-NS simulated physical mixture and plain CAM. (b) X-ray diagrams of crystalline NS at different b-CD/cross-linking agent ratio.

no longer crystalline and confirms its interaction with the NS structure. On the contrary, the binary physical mixtures presented the melting peak of the drug, indicating that CAM maintained its original crystallinity in the physical mixtures due to a lack of interaction (data not shown).

TEM studies showed that the regular spherical shape and sizes of nanosponges (Fig. 6a) that are unaffected even after drug encapsulation (Fig. 6b).

The paracrystalline NS have larger average diameter than the crystalline ones. TEM measurements revealed mean particle size of about 400 nm and 900 nm for plain crystalline and paracrystalline nanosponges, respectively, and a size increase for the drug-loaded crystalline NS. The results obtained by laser light scattering were in agreement with the TEM studies and showed sizes between 450 nm and 600 nm, for the drug-loaded NS (Table 3).

Considering the drug-loading values and the sizes of the series of NS, we selected only the crystalline ones to determine the *in vitro* release kinetics, the stability and the cytotoxicity of CAM formulations.

The complexation of CAM in NS markedly reduced its release, and the release rate depended on the types of NS. The *in vitro* release experiments showed a prolonged release of CAM from nanosponges over a period of 24 h (Fig. 7). The initial burst effect in the release profiles is probably due to the CAM which is not present in the formulations as inclusion complex, but it is adsorbed or encapsulated as non-inclusion complex on the NS surface. After the

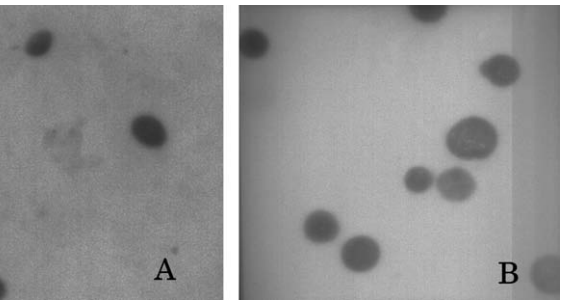

Fig. 6. TEM of (A) blank nanosponges (46,000×) and (B) CAM-loaded nanosponges (46,000×).

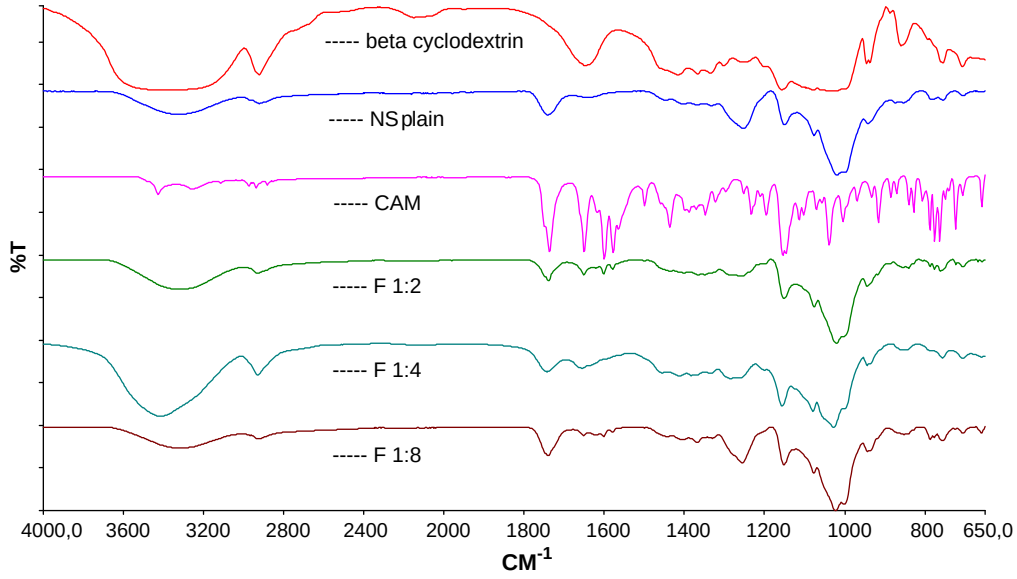

Fig. 5. FTIR spectra of CAM, NS and NS formulations.

Table 3
Characteristics of CAM-loaded NS formulations.

Sr. no.	NS formulation	Average diameter (nm) ± SD	Zeta potential (mV) ± SD	Polydispersity index (PI)
1	$F_{1:2}$	603.4 ± 20.2	−24.90 ± 2.1	0.095
2	$F_{1:4}$	457.4 ± 15.7	−21.55 ± 1.7	0.111
3	$F_{1:8}$	517.7 ± 12.4	−24.70 ± 2.4	0.198
4	F_{para}	907.3 ± 20.3	−20.71 ± 1.8	0.123

initial effect, nearly linear and sustained release profiles of the drug were observed. The differences of the release kinetic values are not statistically significative until 60 min; on the contrary, the release values are statistically different after 60 min until 24 h ($p < 0.05$).

The *in vitro* release of CAM was delayed for the presence of the cyclodextrins in the NS structure when compared to other nanoparticle formulation in which the release kinetics was completed in 24 h [19]. The percentage of CAM released from NS formulations after 24 h ranged between 20% to about 25% showing a strong interaction of the drug with the three types of NS. A similar sustained release profile was obtained with CAM polyrotaxane-based delivery systems, molecular assembly of cyclodextrins [26]. A slow CAM release might decrease the toxic side effects of the drug to the tissues.

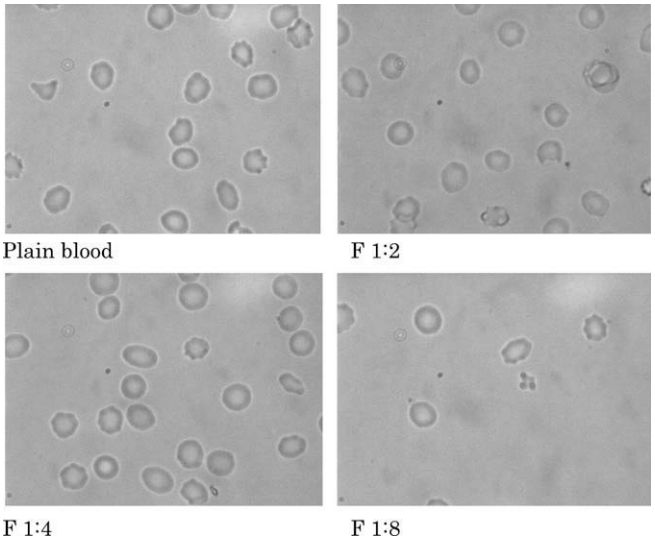

Fig. 9. Erythrocyte stability after incubation with the NS formulations.

The cross-linker amounts in NS affected the release with the following order: $F_{1:4} > F_{1:8} > F_{1:2}$.

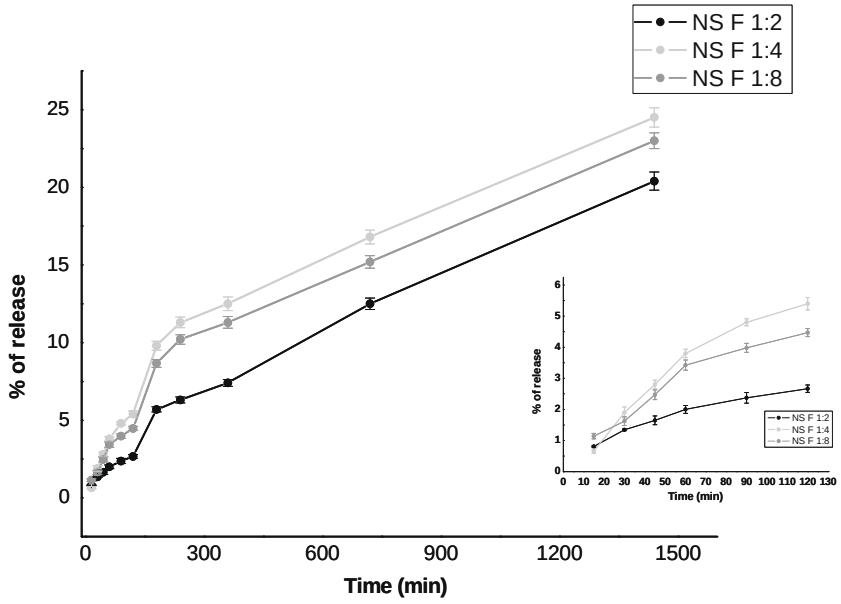

Fig. 7. *In vitro* release profiles of CAM from the three nanosponge formulations.

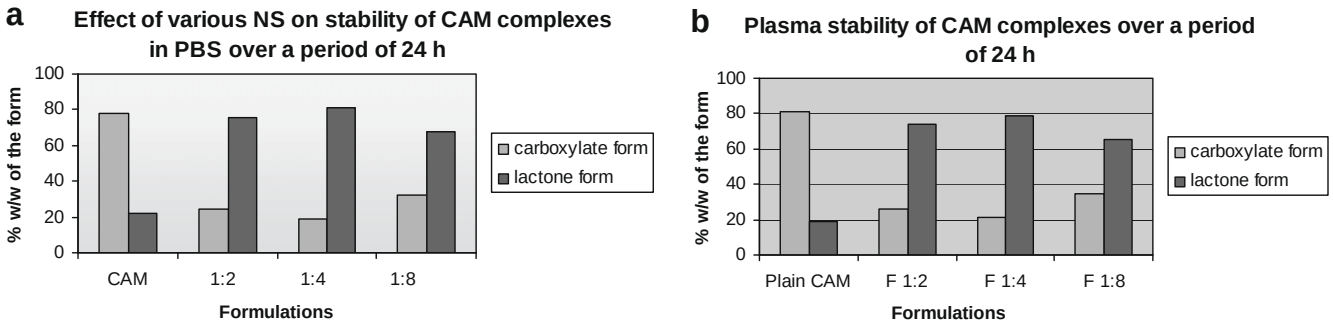

Fig. 8. Plasma stability of the CAM formulations.

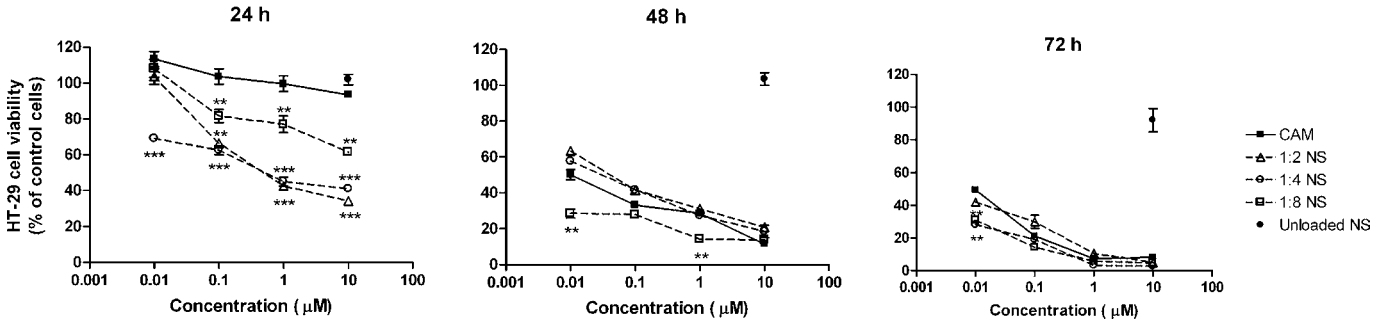

Fig. 10. *In vitro* cytotoxicity of CAM (■), 1:2 NS (Δ), 1:4 NS (○) and 1:8 NS (□) loaded formulations and unloaded NS (●) in HT-29 cells after 24-, 48- and 72-h exposure. Results are mean values ± SD of two independent experiments performed in triplicate. $^{*}p < 0.05$, $^{**}p < 0.01$ and $^{***}p < 0.001$ (CAM vs. loaded NS).

The slowest CAM release from F1:2 than from other formulations might be due to the lowest cross-linking degree which might permit the encapsulation of CAM mainly as inclusion complex in the NS structure.

We suppose that the inclusion of CAM into nanosponges would reduce the possibility of opening the lactone ring of CAM thereby making it more stable as previously observed with cyclodextrin complexation [24].

To confirm this hypothesis, the stability of CAM-loaded in the series of NS was determined either in phosphate buffer pH 7.4 or in plasma after 24 h of incubation at 37 °C (Fig. 8a and b). All the NS formulations were able to protect the drug. At pH 7.4, CAM rapidly converts to the pharmacologically less active carboxylate form. The hydrolysis of CAM was slower when the drug is formulated in nanosponges compared to the plain drug. The lactone form of CAM was markedly higher than the carboxylate one when CAM is encapsulated in all the formulations either in phosphate buffer or in plasma. $F_{1:4}$ formulations seem to be the more protective one (80% of lactone form) confirming the greatest interaction with this type of nanosponges. The complexation favoured the carboxylate/lactone-equilibrium towards the more hydrophobic active lactone form of the drug.

For parenteral administration, the non-toxicity of the formulations is mandatory. To evaluate the safety of the CAM-loaded NS, the haemolytic activity was determined.

The nanosponge aqueous suspensions were non-haemolytic up to the tested concentration of about 20 mg/ml as previously reported [3]. CAM-loaded formulations also showed a good tolerability with erythrocytes; indeed, the amount of haemolysis was negligible, being as much as 99.6–99.7% of erythrocytes intact after incubation with all the nanosponge formulations. Optical microscopy studies confirmed the intactness of the blood cells after incubation with the NS formulations thereby proving its safety (Fig. 9). Thus, the formulations might be considered suitable for parenteral administrations.

Fig. 10 reports the survival curves of HT-29 cells after 24-, 48- and 72-h exposure to CAM, NS and NS formulations, respectively. No significant cytotoxicity of the unloaded nanosponges was observed indicating that the toxicity towards the cells was a consequence of the CAM molecules. Indeed, at the highest concentration tested, the unloaded NS did not decrease the cell viability of HT-29 cells at 24- and 48-h exposure, while a slight decrease was observed at 72-h exposure ($p < 0.05$).

All the NS formulations of camptothecin showed a higher cytotoxic effect with respect to free CAM at 24-h exposure; in particular, $F_{1:4}$ caused the highest decrease in cell growth. On the contrary, CAM, $F_{1:4}$ and $F_{1:2}$ formulations showed a similar inhibitory activity on HT-29 cells at 48- and 72-h exposure, while a higher cytotoxic activity was observed only with $F_{1:8}$ formulation at the lowest concentration used. The increased activity observed for the NS formulations compared to that of free CAM could be partly explained with the increased stability of CAM caused by the interaction with NS because of the complexed CAM is less prone to hydrolysis as previously shown. The lactone ring is essential for passive diffusion of the drug into cancer cells. Moreover, NS might increase the cellular uptake of CAM, as previously observed with fluorescent probes.

4. Conclusions

Cyclodextrin-based NS were able to complex efficiently CAM particularly the crystalline ones. The NS formulations have spherical shape and colloidal sizes. They showed prolonged release profiles and an increased stability of the drug decreasing the hydrolysis of the lactone form in the carboxylate one. Moreover, CAM-loaded formulations showed negligible haemolytic activity and a strong cytotoxicity against HT-29 cells. NS might be proposed as promising carriers for CAM acting as a reservoir for the sustained release of the active form of the drug.

Acknowledgements

The Authors are thankful to Sea Marconi Technologies (Collegno, Italy) for generously funding the research and University of Turinex 60%.

References

[1] F. Trotta, W. Tumiatti, WO 03/085002, 2003.
[2] F. Trotta, R. Cavalli, Characterization and application of new hyper-cross-linked cyclodextrins, Compos. Interfaces 16 (2009) 39–48.
[3] R. Cavalli, F. Trotta, W. Tumiatti, Cyclodextrin-based nanosponges for drug delivery, J. Incl. Phenom. Macrocycl. Chem. 56 (2006) 209–213.
[4] S. Swaminathan, P.R. Vavia, F. Trotta, S. Torne, Formulation of betacyclodextrin based nanosponges of itraconazole, J. Incl. Phenom. Macrocycl. Chem. 57 (2007) 89–94.
[5] P.R. Vavia, S. Swaminattan, F. Trotta, R. Cavalli, Applications of Nanosponges in Drug Delivery XIII International Cyclodextrin Symposium, Turin 14-17, May 2006.
[6] S. Swaminathan, Studies on Novel Dosage Forms, M Pharm. Sci. Thesis, University of Mumbai, India, July 2006.
[7] R.P. Hertzberg, M.J. Caranfa, S.M. Hecht, On the mechanism of topoisomerase I inhibition by camptothecin: evidence for binding to an enzyme–DNA complex, Biochemistry 28 (1989) 4629–4638.
[8] J. Dancey, E.A. Eisenhauer, Current perspectives on camptothecin in cancer treatment, Br. J. Cancer 74 (1996) 327–338.
[9] M. Potmesil, H.M. Pinedo, Camptothecins: New Anticancer Agents, CRC Press, Boca Raton, 1995.
[10] C.H. Takimoto, J. Wright, S.G. Arbuck, Clinical applications of the camptothecins, Biochim. Biophys. Acta 1400 (1998) 107–119.
[11] M.E. Wall, M.C. Wani, C.E. Cook, K.H. Palmer, A.T. McPhail, G.A. Sim, Plant antitumor agents. I. The isolation and structure of camptothecin, a novel alkaloidal leukemia and tumor inhibitor from *Camptotheca accuminata*, J. Am. Chem. Soc. 88 (1966) 3888–3890.
[12] Y.H. Hsiang, R. Hertzberg, S. Hecht, L.F. Liu, Camptothecin induces protein-linked DNA breaks via mammalian DNA topoisomerase I, J. Biol. Chem. 260 (1985) 14873–14878.

[13] J. Fassberg, V.J. Stella, A kinetic and mechanistic study of the hydrolysis of camptothecin and some analogues, J. Pharm. 81 (1992) 676–684.
[14] I. Chourpa, J.M. Millot, G.D. Sockalingum, J.F. Riou, M. Manfait, Kinetics of lactone hydrolysis in antitumor drugs of camptothecin series as studied by fluorescence spectroscopy, Biochim. Biophys. Acta 1379 (1998) 353–366.
[15] T.G. Burke, A.K. Mishra, M.C. Wani, M.E. Wall, Lipid bilayer partitioning and stability of camptothecin drugs, Biochemistry 32 (1993) 5352–5364.
[16] A. Hatefi, B. Amsden, Camptothecin delivery methods, Pharm. Res. 19 (2002) 1389–1399.
[17] A. Scenderova, T. Burke, S. Schwendeman, Stabilization of 10-hydroxycamptothecin in poly(lactide-co-glycolide) microsphere delivery vehicles, Pharm. Res. 14 (10) (1997) 1406.
[18] R. Cortesi, E. Esposito, A. Maietti, E. Menegatti, C. Nastruzzi, Formulation study for the antitumor drug camptothecin: liposomes, micellar solutions and a microemulsion, Int. J. Pharm. 159 (1997) 95–103.
[19] R. Kunii, H. Onishi, Y. Machida, Preparation and antitumor characteristics of PLA/(PEG–PPG–PEG) nanoparticles loaded with camptothecin, Eur. J. Pharm. Biopharm. 67 (2007) 9–17.
[20] M.E. Davis, Design and development of IT-101, a cyclodextrin containing polymer conjugate of camptothecin, Adv. Drug Deliv. Rev. 61 (2009) 1189–1192.
[21] Z. Huang, S. Hua, Y. Yang, J. Fang, Development and evaluation of lipid nanoparticles for camptothecin delivery: a comparison of solid lipid nanoparticles, nanostructured lipid carriers, and lipid emulsion, Acta Pharmacol. Sinica 9 (2008) 1094–1102.
[22] M. Barrada, A. Serreqi, F. Dabbarh, A. Owusu, A. Gupta, S. Lehnert, A novel non-toxic camtothecin formulation for cancer chemotherapy, Biomaterials 26 (2005) 2115–2120.
[23] J. Fang, C. Hung, S. Hua, T. Hwang, Acoustically active perfluorocarbon nanoemulsions as drug delivery carriers for camptothecin: drug release and cytotoxicity against cancer cells, Ultrasonics 49 (2009) 39–46.
[24] J. Kang, V. Kumar, D. Yang, P.R. Chowdhury, R.J. Hohl, Cyclodextrin complexation: influence on solubility, stability and cytotoxicity of camptothecin, Eur. J. Pharm. Sci. 15 (2002) 163–170.
[25] A. Saetern, N. Nguyen, A. Bauer-Brandl, M. Brandl, Effect of hydroxypropyl-β-cyclodextrin-complexation and pH on solubility of camptothecin, Int. J. Pharm. 284 (2004) 61–68.
[26] C. Moon, Y. Kwon, W. Lee, Y. Park, L. Chang, V. Yang, A novel polyrotaxane-based intracellular deliery system for camptothecin: in vitro feasibility, J. Biomedical Mat. Res. Part A 84 (2008) 238–246.